

## Pivotal antitumor role of the immune checkpoint molecule B7-H1 in pancreatic cancer

Alexandr V. Bazhin<sup>a</sup>, Katharina von Ahn<sup>a</sup>, Jasmin Fritz<sup>a</sup>, Henriette Bunge<sup>a</sup>, Caroline Maier<sup>a</sup>, Orkhan Isayev<sup>b</sup>, Florian Neff<sup>c</sup>, Jens T. Siveke<sup>c,d</sup>, and Svetlana Karakhanova<sup>a</sup>

<sup>a</sup>Department of General, Visceral and Transplantation Surgery, University of Heidelberg, Heidelberg, Germany; <sup>b</sup>Department of Cytology, Embryology and Histology, Azerbaijan Medical University, Baku, Azerbaijan; <sup>c</sup>Division of Solid Tumor Translational Oncology, German Cancer Research Center (DKFZ) and German Cancer Consortium (DKTK), partner site University Hospital Essen, Heidelberg, Germany; <sup>d</sup>Bridge Institute of Experimental Tumor Therapy, West German Cancer Center, University Hospital Essen, University Duisburg-Essen, Essen, Germany

### Abstract

Immune checkpoint molecule B7-H1 plays a decisive immune regulatory role in different pathologies including cancer, and manipulation of B7-H1 expression became an attractive approach in cancer immunotherapy. Pancreatic cancer (PDAC) is characterized by pronounced immunosuppressive environment and B7-H1 expression correlates with PDAC prognosis. However, the first attempts to diminish B7-H1 expression in patients were not so successful. This points the complicity of PDAC immunosuppressive network and requires further examinations. We investigated the effect of B7-H1 deficiency in PDAC. Our results clearly show that partial or complete B7-H1 inhibition *in vivo* led to reduced tumor volume and improved survival of PDAC-bearing mice. This oncological benefit is due to the abrogation of immunosuppression provided by MDSC, macrophages, DC and Treg, which resulted in simultaneous restoration of anti-tumor immune response, namely improved accumulation and functionality of effector-memory CD4 and CD8 T cells. Our results underline the potential of B7-H1 molecule to control immunosuppressive network in PDAC and provide new issues for further clinical investigations.

### ARTICLE HISTORY

Received 1 March 2021  
Revised 10 February 2022  
Accepted 10 February 2022

### KEYWORDS

B7-H1 (PD-L1); B7-H1 knockout; immune checkpoint molecules; immunosuppression; cancer immunotherapy; pancreatic cancer

## Introduction

Immunotherapy has become nowadays a paradigm-shifting approach for patients with advanced malignancies. Particularly, the so-called immune checkpoint molecules (ICPM) attract an enormous attention of scientists and clinicians due to the fact that immunotherapy using antibody or inhibitors targeting these molecules could demonstrate spectacular clinical responses.<sup>1</sup> These exciting results led to the approval of antibody against cytotoxic T-lymphocyte-associated protein 4 (CTLA-4), programmed cell death protein 1 (PD-1), and programmed cell death-ligand 1 (PD-L1, B7-H1) for treatment of patients with melanoma, non-small cell lung cancer, and renal cell carcinoma.<sup>2</sup> Unfortunately, only restricted cohorts of patients benefit from these treatments probably due to an intricate network of strong immunosuppression.<sup>3</sup> Pancreatic ductal adenocarcinoma (PDAC) is one of such malignancies, which have not responded to therapies with ICPM inhibitors in pilot clinical trials.<sup>4</sup>

The regulatory cell-surface proteins of the B7-H family play an important role in the modulation of immune responses.<sup>5</sup> B7-homologue 1 (B7-H1, CD274, PD-L1), a ligand for PD-1 receptor, was described by Dong.<sup>6</sup> B7-H1 expression has been found on the surface of macrophages, dendritic cells (DC), and activated T cells, B cells, endothelial, and epithelial cells.<sup>7</sup> Moreover, B7-H1 is ubiquitously present in tumor cells in different types of cancer,<sup>8</sup> and its expression correlates with a poor prognosis for the patient and contributes to tumor

immune evasion.<sup>9</sup> This makes B7-H1 and its regulation an important target for ongoing investigations in the field of cancer immunotherapy, with ICPM inhibitors.

B7-H1-deficient mice (B7-H1KO) were generated by Dong and colleagues.<sup>10</sup> In our recent research, we deeply investigated this mouse strain and showed that B7-H1 deficiency *in vivo* modulates several immunological parameters, including the amount and composition of Gr1<sup>+</sup>CD11b<sup>+</sup> myeloid population, the composition and activation state of the DC compartment, the frequency and status of natural killer (NK) and NKT cells, B cells, naïve/memory state of CD8 T cells, production of IL-2 and IL-10 cytokines, and increased PD-1 expression in the immune cells.<sup>11</sup> All these data underline the importance of B7-H1 as a decisive immune regulatory molecule.

PDAC is one of the deadliest cancers in the world, with 5-year survival rates of only ~1% and median survival of 4–6 months.<sup>12</sup> The reasons for such a poor prognosis are multiple, including rapid tumor dissemination, latent nonspecific symptoms associated with a delayed diagnosis<sup>13</sup> and a highly immunosuppressive milieu.<sup>14</sup> Immunotherapy might be considered as an attractive approach to combat PDAC.<sup>15</sup> However, one phase I trial using an antibody against B7-H1 did not reveal any objective response by the patients,<sup>16</sup> pointing the complicity of immunosuppressive network induced by PDAC. Despite B7-H1 supposed to be one of the crucial actors in this immunosuppressive structure, the immunological outcome of B7-H1 deficiency in PDAC is not fully characterized yet.

In this work, we used both *in vivo* and *ex vivo* approaches to inhibit B7-H1 and demonstrated that such inhibition indeed reduces tumor volume and improves survival of PDAC-bearing mice. This oncological benefit was due to the abrogation of general immunosuppression and simultaneous restoration of an antitumor immune response.

## Materials and methods

### Materials

Antibodies used are listed in the Suppl. Table 1. FoxP3 staining Buffer Set was purchased from eBioscience. Collagenases III and IV and Trypan Blue 0.5 % were obtained from Biochrom AG. DNase I was purchased from Roche. Dulbecco's PBS Solution (10x), HBSS Buffer, and RPMI 1640 were obtained from PAA Laboratories GmbH. RBC Lysis Buffer (10x) was purchased from BioLegend and Hyaluronidase by Linaris GmbH. CD11b MicroBeads as well as Myeloid-Derived Suppressor Cell Isolation mouse kit were purchased by Miltenyi Biotec GmbH. Milliplex<sup>®</sup> MAP Kit, Mouse Cytokine/Chemokine Magnetic Bead Panel, was purchased from EMD Millipore Corporation Merck KGaA. FluoSpheres<sup>®</sup>Carboxylate, Yellow-green (505/515) conjugated, was obtained from Life Technologies. CFSE (5-(and6)-Carboxyl-fluorescein diacetate succinimidyl ester, CFDA SE) and CD274 (B7-H1) Functional Grade Purified antibody were purchased from eBioscience.

### Mice

Two mouse strains in the age range 8–12 weeks were used. The C57BL/6 wild-type mice were purchased by Charles River, Sulzbach. The B7-H1KO mice were originally created by Dong and colleagues by homolog recombination in embryonic stem cells in a C57/Bl6 background<sup>10</sup> and kindly provided by Dr. Linda Diehl and Dr. Percy Knolle. The mice were kept in the animal facility of University Heidelberg (IBF, Heidelberg) and in the Department of Neuropathology (University Hospital, LMU Munich) under specific pathogen-free (SPF) conditions. Homozygous B7-H1KO mice were checked for the KO genotype stability in regular intervals. Experiments with animals were carried out after approval by the authorities (Regierungspraesidium Karlsruhe and Regierungspraesidium Oberbayern).

### Orthotopic mouse model

The murine PDAC model has been induced as previously described.<sup>17</sup> The i.p. treatment with anti-B7-H1 antibody or IgG control (Functional Grade purified B7-H1 and IgG control Ab, eBioscience; 150 µg/mouse in 150 µl) was performed at day (d) 5, 8, 11, 15, 19 after cancer cell transplantation. All *in vivo* primary results were obtained from repetitive independent experiments, and “n” reflects total amount of mice per group. Each *in vivo* experiment data is shown in Suppl. Figure S1.

### Preparation of tumor, spleen, and blood samples

Four weeks after the cell implantation, the mice were sacrificed by cervical dislocation. Spleens and tumors were dissected, and the size was determined using a slide vernier caliper. The abdomen was examined for the presence of metastasis in the liver, intestines, and peritoneum, as well as any adhesions or abnormalities. The size of the metastasis was graded from + to ++++. Blood was allowed to clot and centrifuged at 600 g for 25 min. The clear serum supernatant was centrifuged at 9300 g for 10 min and frozen at –20°C.

### Preparation of a single-cell suspension

Isolated tumors were cut into small pieces and incubated in 5 ml of the collagenases digestion solution at 37°C. Tissue was pressed through a 100 µm cell strainer and flushed with 10 ml of PBS. The samples were centrifuged at 4°C, 400 g, 5 min, and the supernatant was discarded. After adding 1 ml of erythrolysis buffer, the samples were resuspended, incubated for 2 min, and 10 ml of PBS was added to stop erythrolysis. After another centrifugation step, the cells were resuspended in 10 ml of PBS and flowed twice through a 40 µm cell strainer. The cell concentration was adjusted to the  $2 \times 10^6$  cells/50 µl.

### Immunophenotyping with FACS

The splenocytes and tumor cells were stained with different antibody combinations in several panels. In tumor-bearing mice, CD45 antibody was used to differentiate between tumor cells (CD45<sup>−</sup>) and tumor-infiltrating leukocytes (CD45<sup>+</sup>). CD4/CD8 panel: CD4/CD8 T cells as well as their subsets, naïve T cells (CD62L<sup>+</sup>CD44<sup>−</sup>), effector T cells (CD62L<sup>−</sup>CD44<sup>−</sup>), central memory T cells (CD62L<sup>+</sup>CD44<sup>+</sup>), and effector memory T cells (CD62L<sup>−</sup>CD44<sup>+</sup>) were analyzed. DC panel: conventional DC (CD11c<sup>high</sup>CD11b<sup>+</sup>, cDC) and plasmacytoid DC (CD11c<sup>int</sup>CD45R<sup>+</sup>, pDC) were characterized, and the expression of MHC-II (I-A[b]), B7-H1, and CD80 and CD86 molecules was investigated. For the analysis of suppressive cell populations, the Treg panel and the MDSC (Myeloid-derived suppressor cells) panel were used. Treg panel: the T regulatory cells were gated as Foxp3<sup>+</sup>CD25<sup>+</sup> within the CD4 T-cell population. Total MDSC were gated as CD11b<sup>+</sup>Gr1<sup>+</sup>. The granulocytic MDSC are characterized as Ly6C<sup>low</sup>Ly6G<sup>+</sup> and the monocytic MDSC as Ly6C<sup>high</sup>Ly6G<sup>−</sup>. To test functional status of MDSC, the expression of Arginase-1 (Arg-1) and inducible Nitric Oxide Synthase (iNOS) was examined.

To assess phagocytosis activity of macrophages (Gr1<sup>−</sup>/CD11b<sup>+</sup> F4/80<sup>+</sup> cells), Gr1<sup>−</sup>/CD11b<sup>+</sup> cells were isolated in two MACS-isolation steps, using Gr1-negative- followed by CD11b-positive selection. Isolated cells were incubated for 1 h at 37°C with the FluoSpheres<sup>®</sup>Carboxylate yellow-green beads (Life Technology), at a concentration of  $7.7 \times 10^5$  beads/ $1 \times 10^6$  cells and examined by flow cytometry. The amount of phagocytized beads was assessed by analyzing the fluorescence intensity of the cells in the FITC channel. For the detailed gating strategy, see Suppl. Figure S2A.

### Extracellular staining

The cells were preincubated for 10 min with anti-CD16/CD32 mixture, and appropriate antibodies for cell surface molecules were added to 50  $\mu$ l of the cell suspension and incubated for 15 min at 4°C in the dark. The samples were washed twice, resuspended in stain buffer, and analyzed on the BD Canto II Flow cytometer.

### Intracellular staining

First, extracellular staining with non-conjugated antibodies was performed and the cells were fixed with 1 ml of the Fixation/Permeabilization Buffer. The samples were then incubated for at least 3 hours at 4°C in the dark. Afterwards, two washing steps with Permeabilization Buffer were performed at 4°C, 400 g, 5 min and the intracellular and the conjugated extracellular antibodies were pipetted to the samples. After two washing steps with Permeabilization Buffer, the cells were resuspended in stain buffer and analyzed on the BD FACS Canto II.

### MACS (Magnetic Activated Cell Sorting)

MACS separation was performed as described elsewhere,<sup>17</sup> according to manufacturer instructions. For MDSC isolation, Gr1<sup>high</sup>Ly6G<sup>+</sup> cells were magnetically labeled by Anti-Ly6G-Biotin antibody and Anti-Biotin MicroBeads. The first flow-through was pre-enriched in Gr1<sup>dim</sup>Ly6G<sup>-</sup> cells. The positive cells from the column were removed from the outside magnetic field using the MACS buffer and a plunger. To increase the purity of Gr1<sup>high</sup>Ly6G<sup>+</sup> cells, the cells were passed through using a new column. The first flow-through pre-enriched in Gr1<sup>dim</sup>Ly6G<sup>-</sup> cells was further labeled with Anti-Gr1-Biotin antibodies and Streptavidin MicroBeads to isolate Gr1<sup>dim</sup>Ly6G<sup>-</sup> cells by positive selection. For macrophage isolation, Gr1<sup>+</sup> cells were magnetically labeled by Anti-Gr1-Biotin antibody and Anti-Biotin MicroBeads and removed from the suspension by positive selection. The Gr1<sup>-</sup> cells in the first flow-through from the column were subsequently labeled by Anti-CD11b- MicroBeads. To increase the purity of Gr1<sup>-</sup>CD11b<sup>+</sup> cells, they were run through a new second column.

### Co-cultures

The CFSE-labeled splenocytes were seeded at a concentration of  $2 \times 10^5$ /200  $\mu$ l medium and with the cells of interests in 96-well round bottom plates. One hour later, CD3 antibody (1  $\mu$ g/ml) and CD28 antibody (2  $\mu$ g/ml) were added to activate the cells. After 72 hours at 37°C, the supernatant was collected and stored at -20°C for the Luminex assay. The cells were harvested, stained with appropriate antibodies, and analyzed by flow cytometry.

### LUMINEX (Bioplex) assay

LUMINEX assay was performed as described elsewhere,<sup>18</sup> according to the manufacturer instructions, and measured by the Luminex® 100/200 System.

### Statistical analysis

All statistical analyses were performed using GraphPad Prism Version 5.01 or 7.01. Distributions of continuous variables were described by means, SE, median, 25% and 75% percentiles, and were presented as indicated in the Figure Legends. D'Agostino and Pearson omnibus normality tests were conducted to estimate the distribution of data. The null hypothesis (mean values were equal) versus the alternative hypothesis (mean values were not equal) was tested by unpaired, two-tailed *T*-test for normal distributed variants or by the Mann-Whitney test for nonparametric distributed data. Survival analysis was done with Kaplan-Meier curves and statistically analyzed with the Log-rank test. All statistical tests were two-tailed. The significance level was  $\alpha = 5\%$ .

### Results

In this work, we used two approaches for B7-H1 inhibition based on the Panc02 orthotopic model of PDAC. This model is characterized by strong immunosuppression,<sup>17,19</sup> which makes it similar to human PDAC.

For the first approach, the murine PDAC cells of the Panc02 cell line were orthotopically injected in the B7-H1KO mice or in the wild-type (WT) animals (control). For the second one, only WT mice were used for Panc02 cell injection. In this case, one group of the animals was treated with an antibody against B7-H1 and another group became an isotype antibody (control).

Notably, both cultured PDAC Panc02 cells and the tumors generated from the orthotopic injection of Panc02 cells demonstrated the expression of B7-H1 molecule (Suppl. Figure S2B).

### Absence of B7-H1 reduces tumor volume and appearance of peritoneal carcinosis and improves survival of PDAC-bearing mice

First, B7-H1KO and WT BL6 animals (co) were transplanted orthotopically with Panc02 cells, and tumor volume, metastases, and survival of the tumor-bearing mice were analyzed (Figure 1). B7-H1KO mice showed a decrease in the PDAC tumor volume and a reduction of peritoneal carcinosis (Figure 1A and C). No difference in liver and colon metastases was observed (Suppl. Figure S3). Importantly, B7-H1KO tumor-bearing mice demonstrated a clear survival benefit compared to the WT animals (Figure 1B). For the second approach, we operated WT mice and treated them with a monoclonal antibody against B7-H1 (abB7-H1) or with an isotype control IgG (co). The abB7-H1 treatment reduced tumor volume and improved survival of PDAC-bearing mice (Figure 1D and E). We detected also a decrease in a number of liver metastasis, but the difference was not significant (Suppl. Figure S3). Thus, inhibition of B7-H1 leads to an improvement of oncological parameters of PDAC-bearing hosts.

We supposed that the oncological improvement in PDAC-bearing mice observed was due to a restoration of the antitumor immune response. To prove or disprove this hypothesis, a profound investigation of antitumor immunity in the PDAC-bearing mice has been carried out.

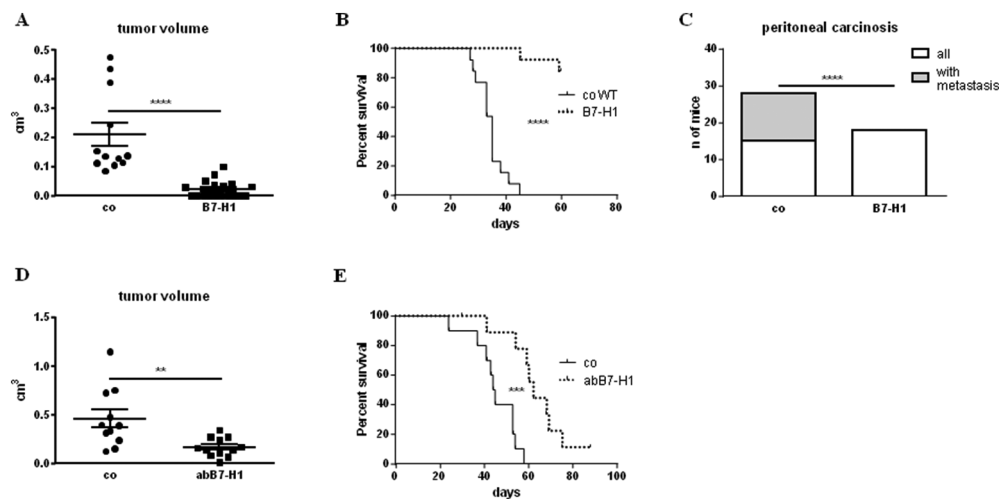


**Figure 1.** Absence of B7-H1 reduces tumor volume and appearance of peritoneal carcinosis and improves survival of PDAC-bearing mice. (A) Tumor volume, (B) survival, and (C) signs of peritoneal carcinosis of WT (co) and B7-H1KO (B7-H1) tumor-bearing mice; (D) tumor volume and (E) survival of WT tumor-bearing mice treated with an antibody against B7-H1 (abB7-H1) or with an isotype control (co). Data are presented (A and D) as a scatter plot (mean with SD),  $n = 11-18$ , analyzed with the unpaired  $T$ -test; (C) as stacked bars analyzed with the fisher's exact test; (B and E) with a Kaplan-Meier curves and analyzed with the log-rank (mantel-cox) test. \*\* $p < 0.01$ , \*\*\* $p < 0.001$ , and \*\*\*\* $p < 0.0001$ .

### Inhibition of B7-H1 leads to a partial abrogation of immunosuppression

As we showed previously, tumors of the Panc02 PDAC model are strongly immunosuppressive due to the tumor accumulation of high amount of Treg and MDSC,<sup>17,19</sup> as well as due to a building of an immunosuppressive cytokine milieu.<sup>18</sup> Thus, we investigated pro- and anti-inflammatory cytokines in the serum of tumor-bearing mice studied in the previous section. In the sera of B7-H1KO PDAC-bearing mice, we detected less VEGF as well as a trend to diminished production of KC (CXCL1) and IL10 (Suppl. Figure S4). Amount of IL1b, TGF $\beta$ , IL4, IL6, and IL13 were not changed significantly (Suppl. Figure S4). Interestingly, in the serum of PDAC-bearing mice treated with the B7-H1 antibody, we could in addition detect a significant decrease in the TGF $\beta$  concentration (Suppl. Figure S4). These results reflect a lower level of immunosuppression on the cytokine level in the tumor-bearing hosts without B7-H1.

At the next step, we profoundly investigated immunosuppression on the cellular level in the tumor-bearing mice with or without B7-H1 expression. We found less Treg in tumors of B7-H1KO mice and in WT PDAC-bearing animals treated with abB7-H1 (Figure 2A and Suppl. Figure S2A). It should be noted that in spleen, we could not see any difference in the Treg amount between the mouse strains analyzed (data not shown). Also an analysis of Tumor Infiltrating Leukocytes (TILs) did not reveal any change in the amount of MDSC (Suppl. Figure S5). However, splenocytes from the tumor-bearing mice demonstrated a decrease in the amount of MDSC in B7-H1KO mice as well as in WT PDAC-bearing animals treated with antibody against B7-H1 (Figure 2B and Suppl. Figure S2A). It is important to note that granulocytic MDSC (gMDSC) was more often detected in TILs of WT tumor-bearing mice compared to B7-H1KO animals, whereas monocytic MDSC (mMDSC) was prominently found in TILs of B7-H1KO mice (Figure 2C and Suppl. Figure S2A). Besides, based on the downregulation of their inducible nitric

oxide synthase (iNOS) and Arginase (Arg) expression, B7-H1KO MDSC have to possess a low immunosuppressive capacity (Figure 2D and Suppl. Figure S2A). Indeed, a proliferation assay using T-lymphocytes as target cells revealed that MDSC from WT mice are stronger immunosuppressive than MDSC from B7-H1KO mice (Figure 3A and Suppl. Figure S2A).

Thus, the general PDAC immunosuppression depends on the status of B7-H1 expression manifesting in modulation of Treg and MDSC as well as their immunosuppressive function.

Since MDSC express high amount of B7-H1 (Figure 3B), it was intriguing to investigate whether this immunosuppressive molecule could reinforce the immunosuppressive effect of these cells. We performed once more a proliferative assay, as mentioned above, using MDSC isolated from WT mice and incubated them with T lymphocytes with or without an antibody against B7-H1. We registered no effect of the antibody on proliferation (data not shown). However, the addition of anti-B7-H1 antibody *in vitro* led to an increase in the interferon- $\gamma$  (IFN $\gamma$ ) concentration in the co-culture supernatants (Figure 3C), indicating that B7-H1 seems to be partially involved in the immunosuppression by MDSC in these experimental settings. Thus, B7-H1 could be engaged in the interplay of MDSC and T cells.

### Inhibition of B7-H1 leads to a restoration of the antitumor immune response in PDAC-bearing mice

We supposed that low level of immunosuppression in B7-H1KO tumor-bearing mice can lead to the restoration of the antitumor immune response, which can be responsible for a better oncological outcome of tumor-bearing animals. Therefore, we investigated in detail lymphocyte populations generally involved in the antitumor response. For this purpose, T cells and their subgroups were analyzed both in spleen and tumor of WT and B7-H1KO tumor-bearing mice. The analysis revealed a high amount of CD4<sup>+</sup> lymphocytes in spleens of B7-H1KO tumor-bearing animals

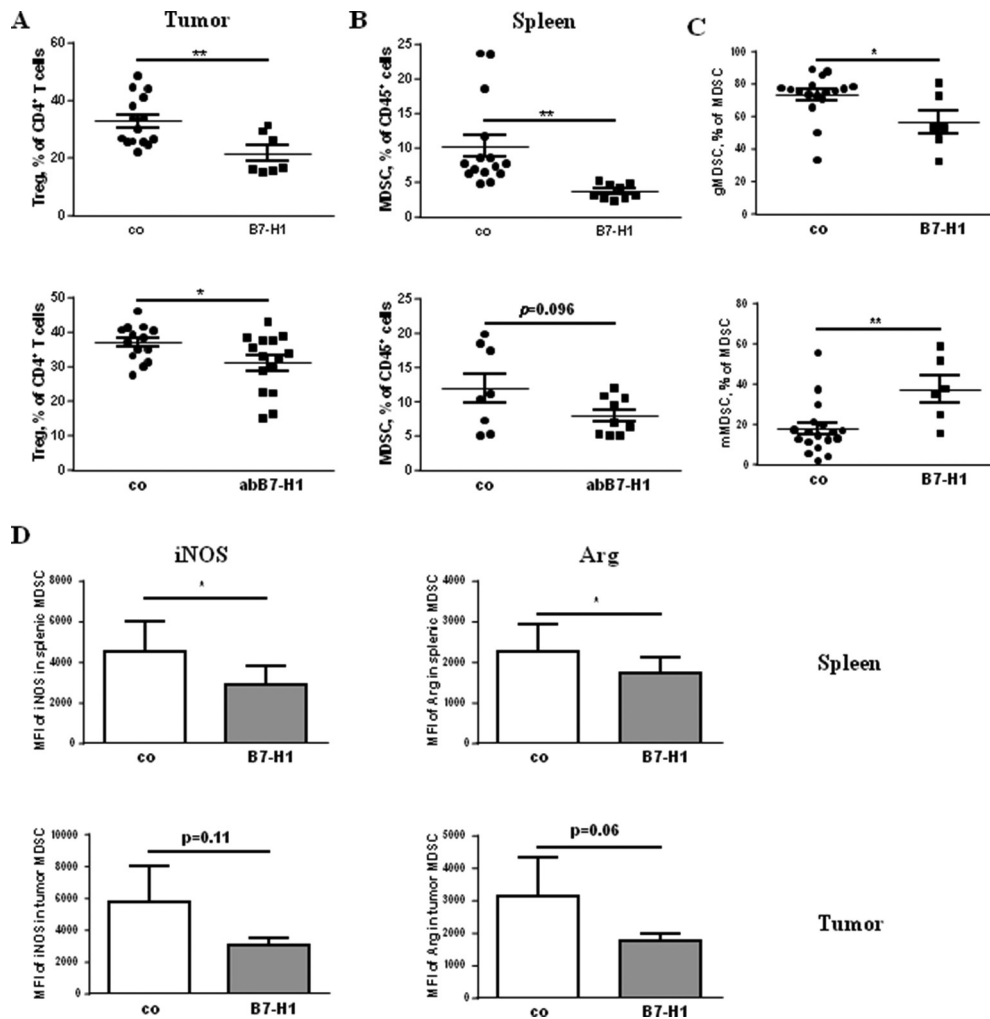


**Figure 2.** Inhibition of B7-H1 leads to a decrease in amount of Treg and MDSC in tumor-bearing mice. (A) Amount of Treg is diminished in the tumor of B7-H1KO mice (B7-H1) and of WT mice treated with antibody against B7-H1 (abB7-H1); data are presented as a scatter plot (mean with SD),  $n = 7-15$ , analyzed with the unpaired  $T$ -test. (B) Amount of MDSC is diminished in the spleen of B7-H1KO mice (B7-H1) and of WT mice treated with antibody against B7-H1 (abB7-H1); data are presented as a scatter plot (mean with SD),  $n = 8-15$ , analyzed with the unpaired  $T$ -test. (C) Distribution of MDSC subpopulations in tumor of mice, data are presented as a scatter plot (mean with SD),  $n = 6-17$ , analyzed with the unpaired  $T$ -test. (D) Expression of iNOS and Arg is lower in the MDSC of B7-H1KO mice (B7-H1); data are presented as a colon bar graph (mean with SD),  $n = 4-12$ , analyzed with the unpaired  $T$ -test. MFI – fluorescence intensity. \* $p < 0.05$ , \*\* $p < 0.01$ .

and in tumors of WT mice (Figure 4A,C and Suppl. Figure S2A). Importantly, a stronger accumulation of effector-memory CD4<sup>+</sup> lymphocytes was detected in the B7-H1KO mice compared to WT animals (Figure 4B and Suppl. Figure S2A). Regarding CD8<sup>+</sup> lymphocytes, their high amount was detected both in tumor and spleen of B7-H1KO animals compared to WT mice (Figure 4D,F and Suppl. Figure S2A). Besides, a pronounced accumulation of effector-memory CD8<sup>+</sup> lymphocytes was found in tumor and in spleen of the B7-H1KO mice (Figure 4E,G and Suppl. Figure S2A). Higher tumoral accumulation of CD8<sup>+</sup> lymphocytes and their effector-memory subpopulation were seen in the WT tumor-bearing mice treated with an antibody against B7-H1, while control treated animals showed lower accumulation of these cells (Suppl. Figure S6). It should be noted that no difference in the B-cell and NK-cell distribution either in tumor or spleen was detected in the tumor-bearing animals investigated (data not shown).

IFN $\gamma$  production by T cells serves as a marker of their activation. Therefore, we measured intracellular IFN $\gamma$  production by TILs and splenocytes obtained from PDAC-bearing WT and B7-H1KO mice. We found higher level of activation of different subpopulation of immune cells in TILs (Figure 5A) and splenocytes (Suppl. Figure S7) isolated from B7-H1KO animals compared to WT ones. Another important antitumor characteristic of immune cells represents the cytotoxicity of TILs against tumor cells. We hypothesized that the TILs from B7-H1KO mice would possess better cytotoxicity than TILs obtained from WT animals. For this purpose, CD45<sup>+</sup> cells were isolated from tumors of both mice strains and co-cultivated with the Panc02 cells. The experiments proved our hypothesis (Figure 5B). The amount of IFN $\gamma$ -producing CD4 and CD8 cells was indeed much higher in the TILs from B7-H1KO tumor-bearing mice as well as the percent of killed tumor cells in the respective co-cultures. This means that abrogation of B7-H1 even only on the non-tumor cells improves antitumor cytotoxicity of TILs.

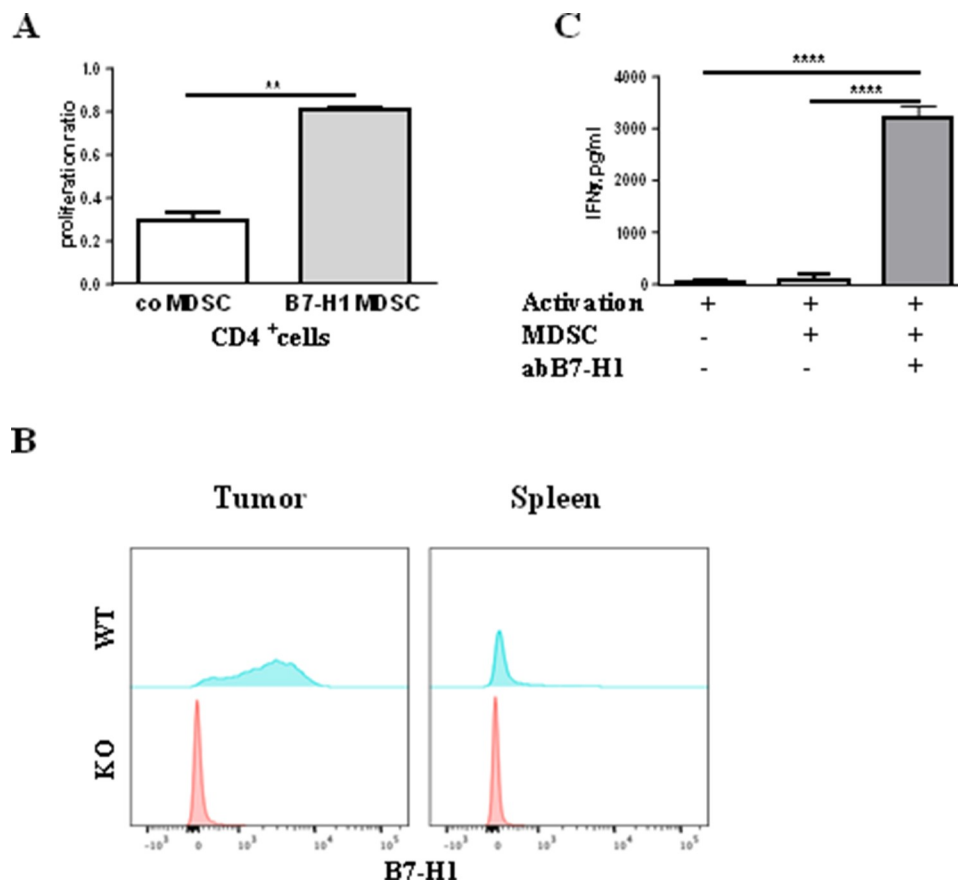


**Figure 3.** MDSC from B7-H1KO tumor-bearing mice are less immunosuppressive as compared to their WT counterparts. (A) MDSC from tumors of B7-H1KO tumor-bearing mice (B7-H1 MDSC) have lower suppressive capacity on the T-cell proliferation than MDSC from tumor of WT tumor-bearing mice (co MDSC). (B) Flow cytometry analysis of the B7-H1 expression on MDSC in tumor and spleen. (C) Analysis of IFN $\gamma$  production by T cells co-cultured with MDSC with or without abB7-H1. A summary of results of two independent experiments, each with 3–5 mouse probes presented as a colon bar graph (mean with SD), analyzed with the unpaired *T*-test. \*\**p* < 0.01 and \*\*\*\**p* < 0.0001.

Thus, the antitumor immune response in the absence of B7-H1 seems to be restored due to higher immune cell activation and improved cytotoxicity, as well as accumulation of effector-memory lymphocyte in the tumor-bearing mice.

#### **Inhibition of B7-H1 improves functionality of DC**

It is well-known that B7-H1 molecule is important for the impeccable function of DC. Therefore, we investigated this immune cell compartment more precisely. While the plasmacytoid (p) DC amount was reduced in the spleen of B7-H1KO tumor-bearing mice compared to the WT ones, these DC showed an improvement in their maturation state (Figure 6A). However, the CD80 co-expression on the surface of pDC was diminished in the absence of B7-H1 (Figure 6A). In regard of CD80 expression on conventional (c) DC, we detected a decrease in the CD80 expression intensity (Figure 6B). Splenocytes of the B7-H1KO tumor-bearing mice showed also an increase in the amount of CD86<sup>+</sup> mature cDC (Figure 6B). However, their expression intensity was reduced (Figure 6B). In addition, in the spleen of mice treated with abB7-H1, a reduction of the cDC amount was registered (Figure 6B). Finally, we saw no phenotypical differences in the

tumor DC of both models (data not shown). Activation and proliferation of CD4<sup>+</sup> lymphocytes after co-incubation with DC serves as a readout for the functionality of DC. Therefore, we isolated DC from tumor and CD4<sup>+</sup> cells from spleen from control WT tumor-bearing mice and co-incubated them with or without an antibody against B7-H1. It should be noted that the antibody alone did not affect the expression of CD69 and CD25 markers on CD4<sup>+</sup> lymphocytes and their proliferation (data not shown). However, blocking of B7-H1 with the antibody in co-cultures led to better activation of lymphocytes (expression of CD69 and CD25) and influenced their proliferation (Suppl. Fig8).

Thus, the inhibition of B7-H1 expression improves the function of PDAC tumor DC.

#### **Inhibition of B7-H1 reduces amount of splenic and tumor M2 macrophages in tumor-bearing mice and induces the macrophage phagocytic activity**

Macrophages play a dual role in tumor-bearing hosts: M1 macrophages are generally involved in antitumor immune response, while M2 favorite tumor progression.<sup>20</sup> In our PDAC model, splenic and tumor macrophages also expressed B7-H1 on their surface (Figure 7A). Therefore,

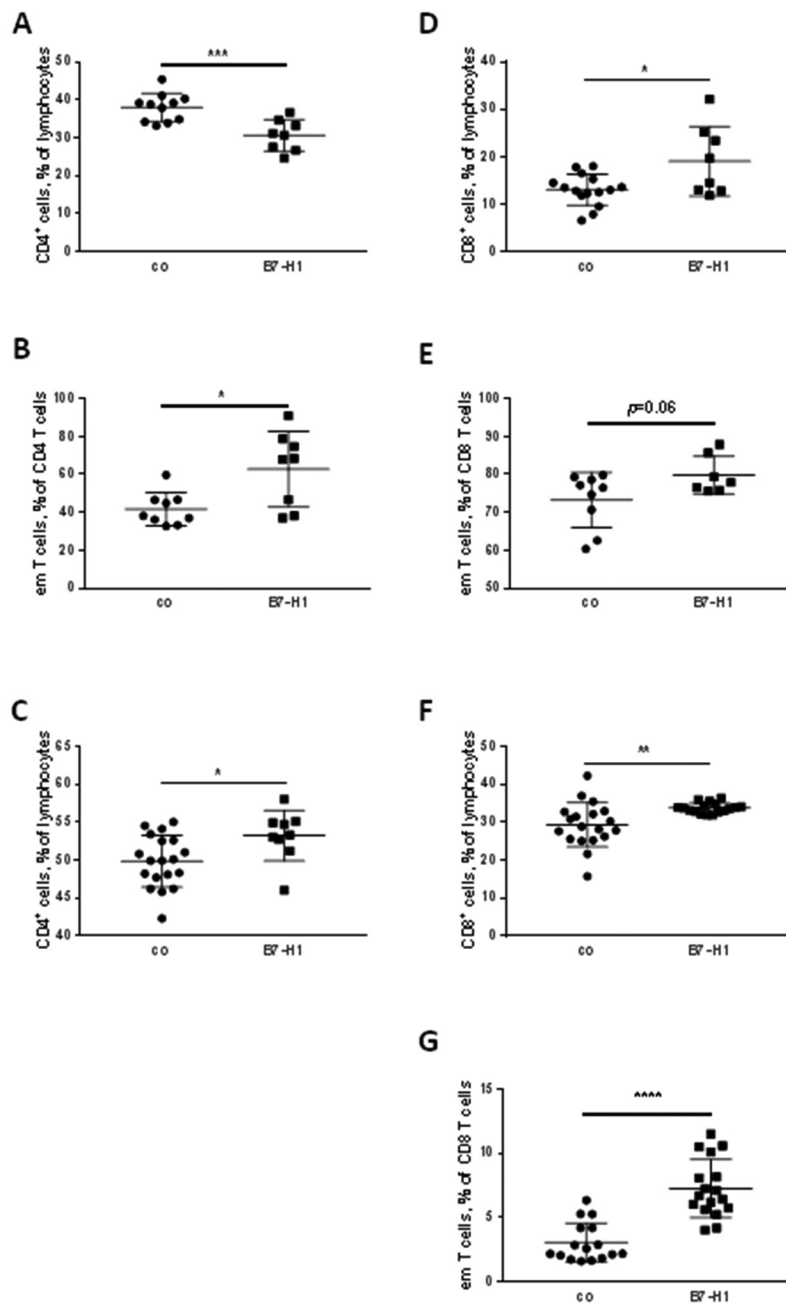


**Figure 4.** Accumulation of effector-memory lymphocytes in the tumor-bearing B7-1KO mice. CD4<sup>+</sup> or CD8<sup>+</sup> lymphocytes in tumor (A and D) and spleen (C and F) and their effector-memory subpopulation (B, E and G). Data are presented as a scatter plot (mean with SD), n = 7–19, analyzed with the unpaired *T*-test. \**p* < 0.05, \*\**p* < 0.01, \*\*\**p* < 0.001, and \*\*\*\**p* < 0.0001.

we questioned whether the B7-H1 inhibition would influence this group of immune cells. We found that the amount of macrophages (CD11b<sup>+</sup>Gr1<sup>-</sup> cells) is decreased in tumor and spleen from B7-1KO mice compared to control WT animals (Figure 7B). Importantly, the amount of M2 (CD206<sup>+</sup>) macrophages was also reduced both in spleen and tumor of the B7-1KO mice (Figure 7B). Since phagocytic activity is an important feature of macrophages, we analyzed it in the tumor macrophages obtained from both tumor-bearing mice strains. Indeed, the macrophages from tumor of B7-1KO mice possessed better phagocytic activity than CD11b<sup>+</sup>Gr1<sup>-</sup> TILs from tumor-bearing WT hosts.

These results suggest that B7-H1 expression is important for macrophages and that the M2 immunosuppressive macrophages are low presented in the absence of this check-point molecule.

### Discussion

In this study, we investigated for the first time in detail the effect of total and partial B7-H1 deficiency in PDAC on the regulation of immune response. Recently, we provided a detailed expression pattern of PD-L1 and its receptor PD-1 on specific healthy mouse immune cells.<sup>21</sup> Taking in account

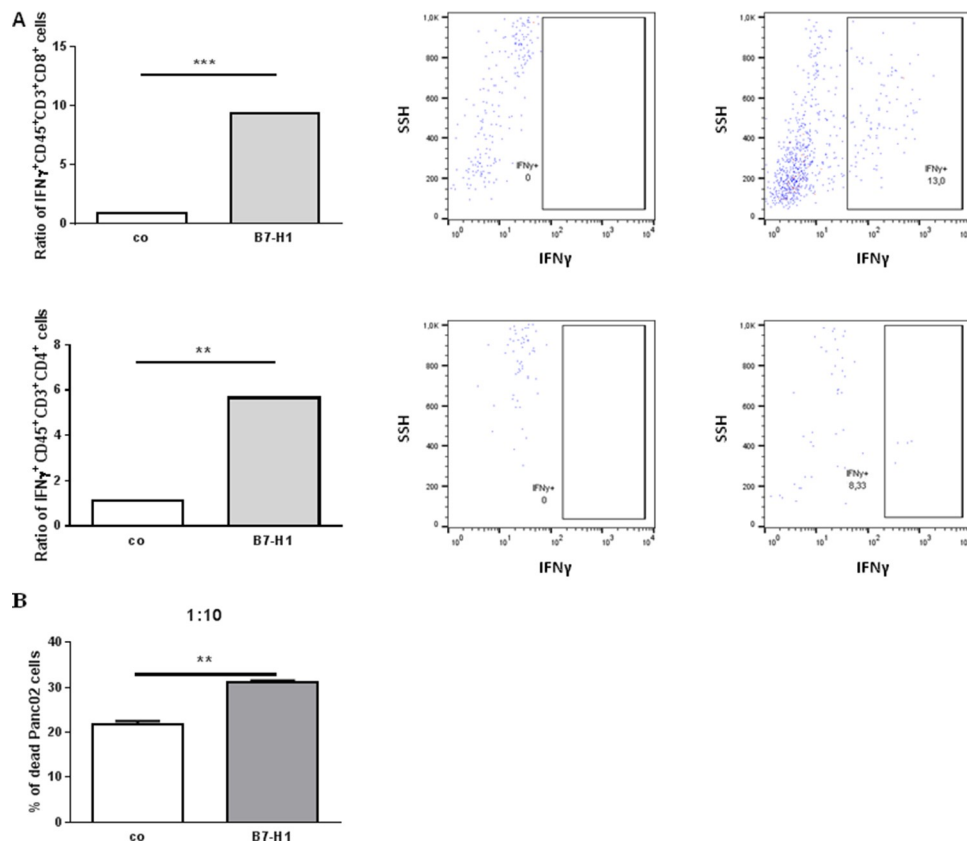


**Figure 5.** Immune cells from tumors of B7-1KO PDAC-bearing mice produce high amount of IFN $\gamma$ . (A) Ratio of intracellular IFN $\gamma$  production in different subpopulation of immune cells (WT (co), B7-1KO (B7-H1)) is presented as a colon bar graph (mean with SD),  $n = 4-8$ , analyzed with the unpaired  $T$ -test – left panel, and as a representative FACS picture – right panel. (B) Cytotoxicity of TILs (WT(co), B7-1KO (B7-H1)) is presented as a percent of cell death in anc02 cells in a colon bar graph (mean with SD) summarizing two independent experiments, each with 3–5 mouse probes, and analyzed with the unpaired  $T$ -test. \*\* $p < 0.01$  and \*\*\* $p < 0.001$ .

the ubiquitous PD-L1 expression demonstrated in this project and in different studies on immune cells like MDSC,<sup>22</sup> macrophages,<sup>23</sup> Treg cells,<sup>24</sup> DC,<sup>25</sup> and of PD-L1 receptor PD-1 on non-myeloid immune cells (CD8, CD4 and Treg),<sup>21</sup> we expected that the absence of B7-1 on immune cell could lead to a decrease in general immunosuppression and consequently to reduced tumor growth.

Indeed, we show here for the first time that the reduction of even only the host non-tumor B7-1 in PDAC leads to the restoration of immune response, tumor reduction, and survival benefit. These results are in line with the recent observations in colon and sarcoma tumor models.<sup>26,27</sup> They also highlight the intriguing discussion about the crucial role of the host immune cells in general and particularly B7-1<sup>+</sup> positive immune cells in the regulation of antitumor response.<sup>28</sup> In our study, the favorable immune effects of B7-1 antibody were surprisingly not more, but sometimes even less pronounced than effects observed in B7-1KO tumor-bearing mice. This implies that aside from various parameters determining the efficacy of immune checkpoint inhibition in PDAC like tumor immunogenicity, initial T-cell priming, immunosuppressive network, and T-cell anergy and exhaustion, some limitations concerning explicit usage of antibody could exist. Antibody delivery to the target tumor and nontumor cells requires not only favorable pharmacokinetics but also sufficient micro-vessel permeability, efficient penetration, and retention in the targeted tissue, which is controlled by

multiple characteristics of antibody and by clinical settings.<sup>29</sup> Moreover, the initial absence of B7-1 molecule in B7-1KO might contribute to the development of more favorable, in context of antitumor response, tumor microenvironment (TME).

Previous reports from Winograd et al. and Ma et al. demonstrated that single anti-PD-1 blockade failed to show anti-cancer activity in murine pancreatic cancer model.<sup>30,31</sup> In the first study, other models of pancreatic cancer were used, namely the KPC mouse spontaneous PDA and the subcutaneous PDA tumor model, which might have a certain differences in organization of TME compared with our orthotopic model.<sup>32</sup> Moreover, in contrast to our approach, anti-PD-1 antibodies were used in both studies to block PD-1/B7-1 axis. Taking in account that (i) PDAC tumor cells express B7-1, (ii) B7-1 expression could be shown on the majority of immune cells, whereby PD-1 expression was more restricted,<sup>21</sup> and (iii) various immune cells expressing B7-1 could be modulated by B7-1 blockage in their phenotypes and functions even in healthy mice,<sup>11</sup> the direct reduction of B7-1 expression might be more encouraging. Besides, B7-1 was described to have an appreciable affinity for the CD80 costimulatory molecule,<sup>33</sup> and recent evidence suggests also that a reverse signaling may exist downstream of B7-1 in both tumor and immune cells.<sup>34</sup> These new B7-1 characteristics are not thoroughly investigated yet, but could make as well an input into the outcome of the direct B7-1 inhibition.

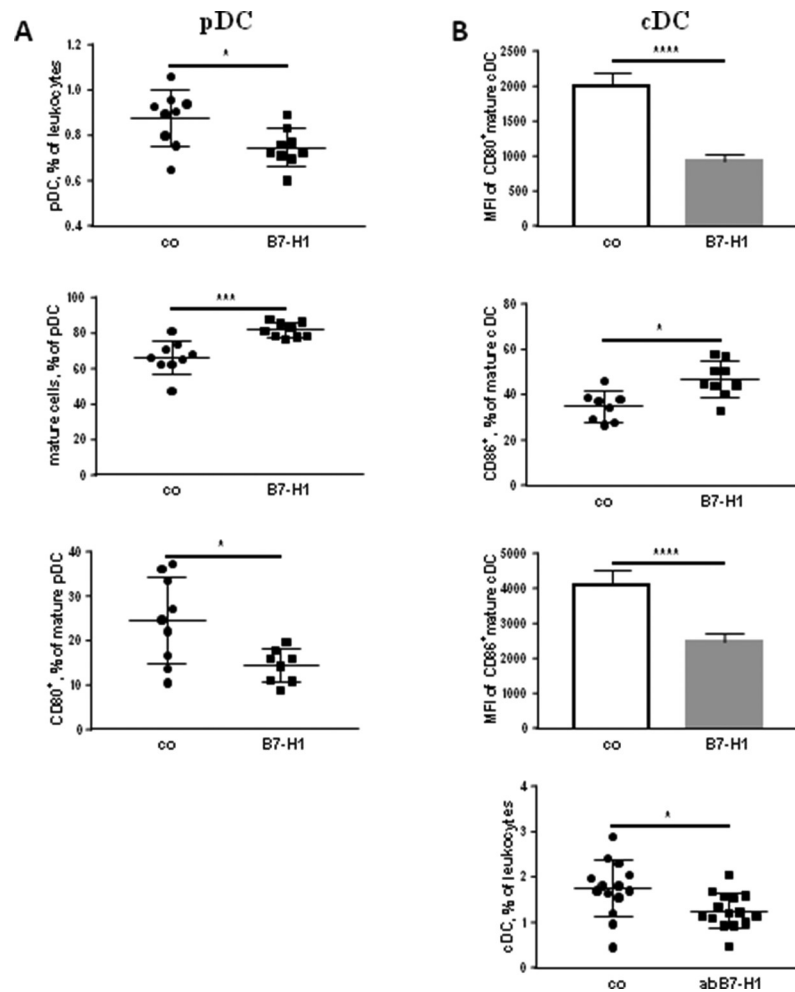


**Figure 6.** B7-H1 has an influence on the composition of splenic DC, their maturation state, and expression of co-stimulatory molecules. Amount of pDC (A) and cDC (B), their maturation state (A and B), and expression of CD80 (A and B) as well as of CD86 (B) molecules on mature DC. WT (co), B7-H1KO (B7-H1), WT treated with antibody against B7-H1 (abB7-H1). (A, B (CD86)) are presented as a scatter plot (mean with SD),  $n = 8-9$ ; amount of cDC (B) presented as a scatter plot (mean with SD),  $n = 14-15$ , and MFI of CD80 and CD86 expression (B) are presented as a column bar graph (mean with SD),  $n = 9$ ; all data are analyzed with the unpaired *T*-test. \* $p < 0.05$ , \*\*\* $p < 0.001$ , and \*\*\*\* $p < 0.01$ .

Our Panc02 PDAC model has several benefits like presence of an intact immune system and of strongly immunosuppressive TME as well as scarcity in effector CD8<sup>+</sup> T cells, making it comparable with human PDAC and suitable for immunotherapeutic preclinical studies. Other sides, this model (i) does not develop a strong desmoplastic reaction and therefore differs in TME and (ii) demonstrates, due to its carcinogen-derived tumorigenesis, a high mutational burden.<sup>32</sup> This may limit the use of Panc02 model in immunotherapeutic approaches, since these characteristics can modulate the efficiency of immunotherapy. For example s.c. Panc02 tumor-bearing mice usually respond better to immune checkpoint blockade.<sup>35,36</sup> In contrast, in the work of Luheshi et al., Panc02 pancreatic tumor cells were surgically implanted in matrigel to produce more robust TME, similar to human PDAC. This study demonstrated that modulation of the TME by a CD40 agonist antibody correlates with improved antitumor reactions to, otherwise, poor responsive, PD-L1 blockade, underlining relevance of TME variations in therapeutic studies.<sup>37</sup>

Since human PDAC has generally lower mutation burden unless it has mismatch repair (MMR) deficiency (d-MMR), the promising results obtained in PDAC model might be

particularly relevant for this cohort of patients. Supportively, d-MMR, including MMR protein loss and/or microsatellite instability, was shown to be predictive of response to immunotherapy in pancreatic cancer.<sup>38</sup>

Recent clinical trials reported no clinical benefit of single agent B7-H1 blockade by antibody Durvalumab in pancreatic adenocarcinoma.<sup>39</sup> However, patients in clinical studies are much more heterogenic than the experimental mice, which are of the same line, age, tumor inoculation time, early injection time of antibody, etc. They often, like in this trial, represent a population of patients with mPDAC who had poor prognoses and rapidly progressing disease. Most of the studies enroll an unselected group of patients to treat, and the number of respondents might appear insufficient to establish the association between clinical outcomes and B7-H1 expression.<sup>39</sup> In line, in recent years in PDAC studies, multiple evaluated targeted therapies and cancer vaccines failed to show efficacy in late-stage clinical trials.<sup>40</sup> Despite preclinical tumor models partially reflect the human disease, the complex tumor environment of PDAC, which is genetically heterogenic, hypoxic, fibrotic, immunosuppressive, and not highly immunogenic, still differs in humans.

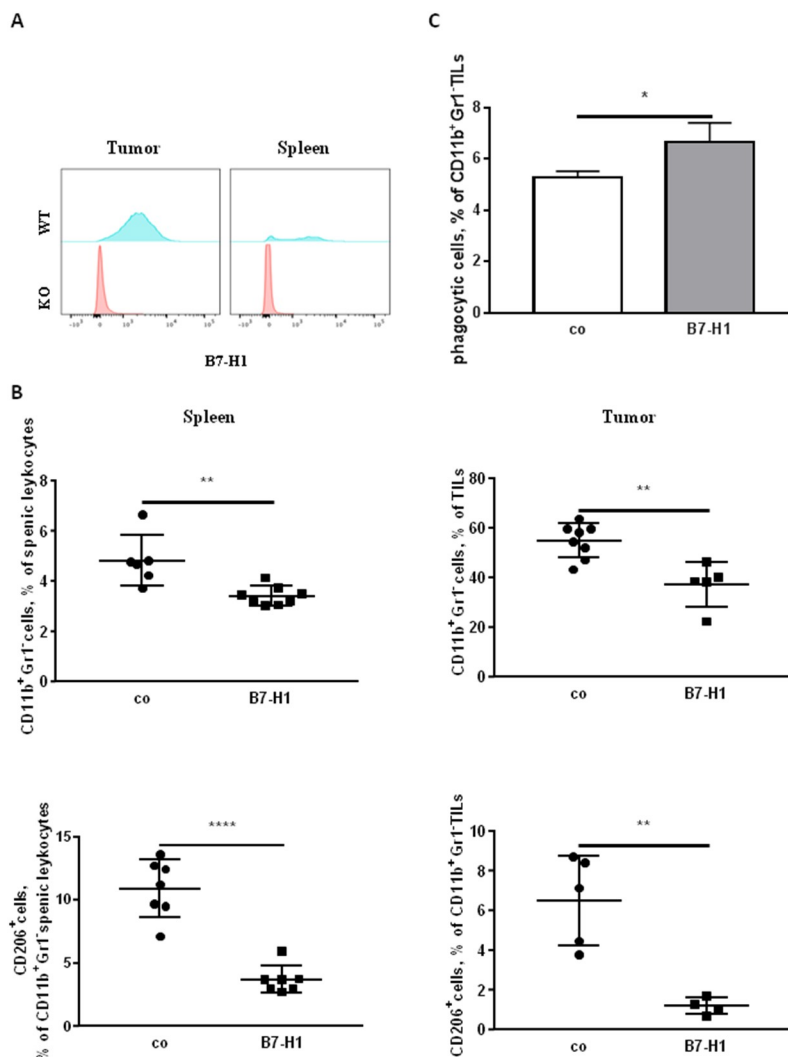


**Figure 7.** Absence of B7-H1 abolishes the accumulation of M2 macrophages. (A) Flow cytometry analysis of the B7-H1 expression on macrophages in tumor and spleen. Representative FACS pictures are shown. (B) Macrophage and M2 macrophage accumulation in spleen and tumor of mice, WT (co), B7-H1KO (B7-H1). Data are presented as a scatter plot (mean with SD),  $n = 4-8$ , analyzed with the unpaired  $T$ -test. (C) Phagocytic activities of macrophages were evaluated as an uptake of fluorescent-labeled beads analyzed by flow cytometry, WT (co), B7-H1KO (B7-H1). Data are presented as a column bar graph summarized from two independent experiments, each with 3–5 mouse probes, and analyzed with the unpaired  $T$ -test. \* $p < 0.05$ , \*\* $p < 0.01$ , and \*\*\*\* $p < 0.0001$ .

Our study clearly demonstrates that B7-H1 inhibition approach has a therapeutic potential, despite disappointing outcome in the first clinical trials. We believe that various parameters and clinical settings should be further examined and optimized in order to achieve in patients similar effects of B7-H1 inhibition on immunosuppressive network and immune response as were observed in our PDAC model. Future studies should as well evaluate the possibilities to identify patients most likely to benefit from B7-H1 inhibition and to develop the best combined therapies with B7-H1 blockade and other agents. Hereby, the simultaneous targeting of other molecular or cellular components of PDAC immunosuppressive network as well as individualized treatment for certain patient populations could be promising approaches.

One of the crucial immunosuppressive axes is provided by MDSC. We demonstrated previously that a decrease in MDSC frequencies and in the systemic VEGF level leads to a restoration of anti-cancer immune responses and an improved survival of PDAC-bearing female mice and hypothesized that MDSC are strongly involved in the PDAC-associated

immunosuppression.<sup>17</sup> Also pancreatic cancer patients with up-regulated B7-H1 display lymphocyte exhaustion and are more enriched in MDSC.<sup>41</sup> In this study, we observed in the sera less VEGF in B7-H1KO. In spleens, we found a decrease in the amount of MDSC in B7-H1KO tumor-bearing mice as well as in WT PDAC-bearing animals treated with antibody against B7-H1. This is also aligned with our foregoing observation that B7-H1KO healthy mice have a reduced Gr1<sup>+</sup>CD11b<sup>+</sup> compartment within myeloid cells<sup>11</sup> and with strong indications that signaling through B7-H1 can make an input in cancer immune escape functionally related to MDSC.<sup>42,43</sup>

Not only the expansion of MDSC but also their iNOS /Arg production and suppressive activity were partially B7-H1-dependent in our study. In accordance, the role of B7-H1 in MDSC function was highlighted in several other models. *In vitro* studies with human gMDSC showed that targeting B7-H1 partially impaired MDSC-mediated T-cell suppression.<sup>43</sup> Human bone marrow-derived B7-H1<sup>+</sup>MDSC are responsible for immune suppression through a mechanism involving Arg-1 and IDO expression, and B7-H1 and MHC class II expression

on *in vitro* produced bone marrow-derived MDSC and MDSC from patients with melanoma and colorectal cancer correlated with T-cell dysfunction.<sup>44</sup> In hepatocellular carcinoma (HCC) patients, higher percentages of B7-H1<sup>+</sup>MDSC was found, which were inversely correlated with disease-free survival and were reduced by HCC treatment.<sup>45</sup> Moreover, the majority of liver MDSC, which are associated with liver metastases and suppress antitumor immunity, express high level of B7-H1 and demonstrate B7-H1-dependent mode of suppression.<sup>46</sup> Also in multiple myeloma, MDSC were characterized by high expression of B7-H1, and PD-1/B7-H1 blockade made an input in the inhibition of MDSC-mediated immune suppression and multiple myeloma growth.<sup>47</sup> Interestingly, age as a known factor encouraging immunosuppression promoted accumulation of B7-H1<sup>+</sup> MDSC in aged mice in lung cancer and enhanced tumor growth. These pro-tumor effects could be diminished by inhibition of B7-H1 with specific antibody.<sup>48</sup> MDSC compartment is divided into two subpopulations, and gMDSC was strongly presented in the WT tumor-bearing mice while mMDSC was predominantly found in the B7-H1KO mice. In contrast, in healthy B7-H1KO mice, the ratio between Gr1<sup>+</sup>CD11b<sup>+</sup>Ly6C<sup>low</sup> and Gr1<sup>+</sup>CD11b<sup>+</sup>Ly6C<sup>high</sup> subpopulations was shifted toward Gr1<sup>+</sup>CD11b<sup>+</sup>Ly6C<sup>low</sup> cells.<sup>11</sup> Which role the ratio between gMDSC and mMDSC could play in general and particularly in anti-cancer immunity is still the matter of debate. However, several observations pointed to the specific characteristics of gMDSC subset. For example, in prostate cancer, gMDSC is supposed to exhibit a high pSTAT3 levels and a high degree of immunosuppressive activity and high levels of B7-H1.<sup>49</sup> Increased levels of gMDSC were also found in individuals with initial phase of HIV infection, which correlated negatively with CD4 T-cell levels. Moreover, this B7-H1 expression was utilized by gMDSC to inhibit proliferation and IFN $\gamma$  secretion of CD8 T cells.<sup>50</sup>

Other closely related myeloid cells – macrophages – were as well reduced in their numbers in tumor and spleen from tumor-bearing B7-H1KO mice, but possessed better phagocytic activity. Tumor-associated macrophages can restrict immune engagement and therefore became an attractive target in PDAC treatment.<sup>51</sup> In PDAC, the high number of macrophages was associated with poor prognosis.<sup>52</sup> Phagocytosis and intracellular killing activity of macrophages in tuberculosis can be as well as significantly increased with PD-1/PD-L1 blockade.<sup>53</sup> Development and progression of oral squamous cell carcinoma are characterized by the augmented presence of M2 macrophages with upregulated B7-H1 expression and correlated with increased capacity to induce T-cell apoptosis.<sup>54</sup>

Particularly important in our experiments is the concomitant reduction of tumor-promoting M2 macrophages in spleen and tumor of B7-H1KO mice, which are an important part of tumor immune suppressive environment<sup>55</sup> and are associated with decreased survival and poor prognosis in pancreatic cancer.<sup>52</sup> Also in gastric adenocarcinoma cells, M2-like macrophage infiltration is highly associated with B7-H1 expression.<sup>56</sup> In this work, we did not investigate other potentially important part of tumor environment, namely cancer-associated fibroblasts (CAFs), which represent a heterogeneous population of cells. Recent studies, however, suggested that in some cancers, CAFs express B7-H1, which can serve as a prognostic marker<sup>57,58</sup> and described a CAF subset that is associated with a poor response

to anti-B7-H1 therapy.<sup>59</sup> Thus, further investigation of interplay between tumor cells, CAFs, and immune cells could explore our knowledge regarding immune checkpoint blockade therapy.

DC is one of the major cell compartments that express B7-H1 and can further up-regulate it in response to various stimuli,<sup>21,25,60</sup> but less is known about the effect of B7-H1 on DC per se. We demonstrated that while in the tumor-bearing mice the pDC subpopulation was reduced in the spleen of B7-H1KO but showed an improvement in their maturation state, in healthy B7-H1KO, the percentage of pDC was increased.<sup>11</sup> In addition, in the spleen of PDAC mice treated with abB7-H1, a reduction of the cDC amount was registered. This means that B7-H1 molecule is involved in the regulation of DC subdivisions, but the outcome is different in case of tumor presence or healthy conditions. The CD80 co-expression on the surface of pDC and cDC was diminished in the absence of B7-H1 in tumor-bearing hosts. In line, the same effect we previously observed in healthy B7-H1KO.<sup>11</sup> Thus, this intrinsic regulation occurs independently from tumor environment. Splenocytes of the B7-H1KO tumor-bearing mice showed in this study an increase in the amount of CD86<sup>+</sup> mature cDC but reduction in the intensity of CD86 expression. Interestingly, the amount of CD86<sup>+</sup> pDC and CD86 expression intensity was higher in B7-H1KO healthy mice, whereas cDC did not demonstrate any variations.<sup>11</sup> So, the modulation of maturation stage upon B7-H1 deficiency seems to be as well partially tumor dependent.

In accordance with the observations of other researchers and our own previous findings discussed, we demonstrated here that B7-H1 expression on DC correlates with their stimulation capacity toward T cells, since the inhibition of B7-H1 expression improves the activation ability of PDAC tumor DC. In our recent work, we showed that DC represented only a small population in PDAC TILs, did not possess tolerogenic phenotype and still could improve the proliferation capacity of the co-cultured splenocytes.<sup>17</sup> This let us assume that DC are not a major player in the context of immunosuppression in PDAC but rather a soft tuner.<sup>17</sup> However, it is known that DC has reduced functions in several types of cancer, including PDAC, and many clinical approaches aim to improve their stimulatory potential.<sup>61</sup>

Another important pivot point of cellular immunosuppression is Treg cells, which are highly enriched in the PDAC.<sup>17,19</sup> Various observations demonstrated that B7-H1 expression could encourage accumulation of Treg and that manipulating of the PD-1/B7-H1 interaction can enhance the *in vitro* and *ex vivo* expansion and function of Tregs.<sup>62–64</sup>

In context of pancreatic tumor, we accordingly found less Treg in tumors of B7-H1KO mice and in WT PDAC-bearing animals treated with abB7-H1, while in healthy B7-H1KO mice, we have rather seen a percentile increase in Treg within the CD4 compartment.<sup>11</sup> These results propose that the absence of B7-H1 can modulate Treg incidental to tumor presence.

Taken together, our findings demonstrate that B7-H1 deficiency affects the most prominent suppression actors in PDAC, by influencing their amount, constellation, and functions. Consequently, we observed restoration of immune response manifested in the increased accumulation of

effector-memory CD4 and CD8 cells and improved functionality of CD4 and CD8 compartments. Our results highlight the great potential of B7-H1 molecule to control sophisticated immunosuppressive network in PDAC. They also provide new impulses for further clinical investigations to improve the immunotherapy with checkpoint B7-H1 inhibition and its clinical outcome.

## Acknowledgments

The authors thank Ms. Tina Maxelon, Ms. Inna Schwarting, Mr. Markus Herbst, and Ms. Michaela Svihla for their excellent technical assistance. This study was supported by Funding Program “Foundations and Prizes” of the Medical Faculty Heidelberg to S.K. The J.T.S. is supported by the German Cancer Consortium (DKTK), the Deutsche Forschungsgemeinschaft (DFG) through grant SI1549/3–1 (Clinical Research Unit KFO337) and SI1549/4–1 and the German Cancer Aid (#70112505/PIPAC, #70113834/PREDICT-PACA).

## Disclosure statement

No potential conflict of interest was reported by the author(s). J.T.S. receives honoraria as consultant or for continuing medical education presentations from AstraZeneca, Bayer, Immunocore, Roche, Servier. His institution receives research funding from Bristol-Myers Squibb, Celgene, Roche; He holds ownership and serves on the Board of Directors of Pharma15, all outside the submitted work.

## Funding

This work was supported by the Funding Program “Foundations and Prizes” of the Medical Faculty Heidelberg to S.K. and work in the lab of J.T.S. is supported by the German Cancer Consortium (DKTK), the Deutsche Forschungsgemeinschaft (DFG; SI1549/3–1 (Clinical Research Unit KFO337), SI1549/4–1); the Deutsche Krebshilfe (German Cancer Aid; #70112505, PIPAC, #70113834, PREDICT-PACA).

## ORCID

Jens T. Siveke  <http://orcid.org/0000-0002-8772-4778>

## Author contributions:

SK and AB participated in the conceptualization and research design; All authors participated in carrying out the research and analyzing the data; AB and SK participated in writing the manuscript and critical correction of the manuscript. AB and SK administered this work. All authors discussed the results and implications and gave constructive feedback on the manuscript at all stages.

## References

- Bazhin AV, Amedei A, Karakhanova S. Editorial: immune checkpoint molecules and cancer immunotherapy. *Front Immunol.* 2018;9(2878). doi:10.3389/fimmu.2018.02878.
- Yan Y, Kumar AB, Finnes H, Markovic SN, Park S, Dronca RS, Dong H. Combining immune checkpoint inhibitors with conventional cancer therapy. *Front Immunol.* 2018;9(1739). doi:10.3389/fimmu.2018.01739.
- Weber R, Fleming V, Hu X, Nagibin V, Groth C, Altevogt P, Utikal J, Umansky V. Myeloid-derived suppressor cells hinder the anti-cancer activity of immune checkpoint inhibitors. *Front Immunol.* 2018;9:1310. doi:10.3389/fimmu.2018.01310.
- Kabacaoglu D, Ciecieski KJ, Ruess DA, Algül H. Immune checkpoint inhibition for pancreatic ductal adenocarcinoma: current limitations and future options. *Front Immunol.* 2018;9:1878. doi:10.3389/fimmu.2018.01878.
- Greaves P, Gribben JG. The role of B7 family molecules in hematologic malignancy. *Blood.* 2013;121(5):734–744. doi:10.1182/blood-2012-10-385591.
- Dong H, Zhu G, Tamada K, Chen L. B7-H1, a third member of the B7 family, co-stimulates T-cell proliferation and interleukin-10 secretion. *Nat Med.* 1999;5(12):1365. doi:10.1038/70932.
- Greenwald RJ, Freeman GJ, Sharpe AH. The B7 family revisited. *Annu Rev Immunol.* 2005;23(1):515–548. doi:10.1146/annurev.immunol.23.021704.115611.
- Dong H, Chen L. B7-H1 pathway and its role in the evasion of tumor immunity. *J Mol Med.* 2003;81(5):281–287. doi:10.1007/s00109-003-0430-2.
- Loos M, Giese NA, Kleeff J, Giese T, Gaida MM, Bergmann F, Laschinger M, W.Büchler M, Friess H. Clinical significance and regulation of the costimulatory molecule B7-H1 in pancreatic cancer. *Cancer Lett.* 2008;268(1):98–109. doi:10.1016/j.canlet.2008.03.056.
- Dong H, Zhu G, Tamada K, Flies DB, van Deursen JMA, Chen L. B7-H1 determines accumulation and deletion of intrahepatic CD8 + T lymphocytes. *Immunity.* 2004;20(3):327–336. doi:10.1016/S1074-7613(04)00050-0.
- Bazhin AV, von Ahn K, Maier C, Solttek S, Serba S, Diehl L, Werner J, Karakhanova S. Immunological in vivo effects of B7-H1 deficiency. *Immunol Lett.* 2014;162(2 Pt B):273–286. doi:10.1016/j.imlet.2014.08.013.
- Werner J, Combs SE, Springfield C, Hartwig W, Hackert T, Büchler MW. Advanced-stage pancreatic cancer: therapy options. *Nat Rev Clin Oncol.* 2013;10(6):323. doi:10.1038/nrclinonc.2013.66.
- Rosty C, Goggins M. Early detection of pancreatic carcinoma. *Hematol Oncol Clin North Am.* 2002;16(1):37–52. doi:10.1016/S0889-8588(01)00007-7.
- Bazhin AV, Shevchenko I, Umansky V, Werner J, Karakhanova S. Two immune faces of pancreatic adenocarcinoma: possible implication for immunotherapy. *Cancer Immunol Immuno.* 2014;63(1):59–65. doi:10.1007/s00262-013-1485-8.
- Bazhin AV, Bayry J, Umansky V, Werner J, Karakhanova S. Overcoming immunosuppression as a new immunotherapeutic approach against pancreatic cancer. *Oncoimmunology.* 2013;2(9):e25736. doi:10.4161/onci.25736.
- Brahmer JR, Tykodi SS, Chow LQM, Hwu W-J, Topalian SL, Hwu P, Drake CG, Camacho LH, Kauh J, Odunsi K, et al. Safety and activity of anti-PD-L1 antibody in patients with advanced cancer. *N Engl J Med.* 2012;366(26):2455–2465. doi:10.1056/NEJMoa1200694.
- Karakhanova S, Link J, Heinrich M, Shevchenko I, Yang Y, Hassenpflug M, Bunge H, von Ahn K, Brecht R, Mathes A, et al. Characterization of myeloid leukocytes and soluble mediators in pancreatic cancer: importance of myeloid-derived suppressor cells. *Oncoimmunology.* 2015;4(4):e998519. doi:10.1080/2162402X.2014.998519.
- Bazhin AV, Yang Y, D’Haese JG, Werner J, Philippov PP, Karakhanova S. The novel mitochondria-targeted antioxidant SkQ1 modulates angiogenesis and inflammatory microenvironment in a murine orthotopic model of pancreatic cancer. *Int J Cancer.* 2016;139(1):130–139. doi:10.1002/ijc.30054.
- Shevchenko I, Karakhanova S, Solttek S, Link J, Bayry J, Werner J, Umansky V, Bazhin AV. Low-dose gemcitabine depletes regulatory T cells and improves survival in the orthotopic panc02 model of pancreatic cancer. *Int J Cancer.* 2013;133(1):98–107. doi:10.1002/ijc.27990.
- Chanmee T, Ontong P, Konno K, Itano N. Tumor-associated macrophages as major players in the tumor microenvironment. *Cancers.* 2014;6(3):1670–1690. doi:10.3390/cancers6031670.
- Bazhin AV, von Ahn K, Fritz J, Werner J, Karakhanova S. Interferon-alpha up-regulates the expression of PD-L1 molecules on immune cells through STAT3 and p38 signaling. *Front Immunol.* 2018;9:2129. doi:10.3389/fimmu.2018.02129.

22. Liu Y, Zeng B, Zhang Z, Zhang Y, Yang R. B7-H1 on myeloid-derived suppressor cells in immune suppression by a mouse model of ovarian cancer. *Clin Immunol.* 2008;129(3):471–481. doi:10.1016/j.clim.2008.07.030.
23. Wagner CJ, Huber S, Wirth S, Voehringer D. Chitin induces upregulation of B7-H1 on macrophages and inhibits T-cell proliferation. *Eur J Immunol.* 2010;40(10):2882–2890. doi:10.1002/eji.201040422.
24. Ghebeh H, Barhoush E, Tulbah A, Elkum N, Al-Tweigeri T, Dermime S. FOXP3(+)/T(regs)and B7-H1(+)/PD-1(+)/T lymphocytes co-infiltrate the tumor tissues of high-risk breast cancer patients: implication for immunotherapy. *BMC Cancer.* 2008;8(1):57. doi:10.1186/1471-2407-8-57.
25. Karakhanova S, Bedke T, Enk AH, Mahnke K. IL-27 renders DC immunosuppressive by induction of B7-H1. *J Leukoc Biol.* 2011;89(6):837–845. doi:10.1189/jlb.1209788.
26. Lau J, Cheung J, Navarro A, Lianoglou S, Haley B, Totpal K, Sanders L, Koepfen H, Caplazi P, McBride J, et al. Tumour and host cell PD-L1 is required to mediate suppression of anti-tumour immunity in mice. *Nat Commun.* 2017;8(1):14572. doi:10.1038/ncomms14572.
27. Noguchi T, Ward JP, Gubin MM, Arthur CD, Lee SH, Hundal J, Selby MJ, Graziano RF, Mardis ER, Korman AJ, et al. Temporally distinct PD-L1 expression by tumor and host cells contributes to immune escape. *Cancer Immunol Res.* 2017;5(2):106–117. doi:10.1158/2326-6066.CIR-16-0391.
28. Tang F, Zheng P. Tumor cells versus host immune cells: whose PD-L1 contributes to PD-1/PD-L1 blockade mediated cancer immunotherapy? *Cell Biosci.* 2018;8(1):34. doi:10.1186/s13578-018-0232-4.
29. Chames P, Van Regenmortel M, Weiss E, Baty D. Therapeutic antibodies: successes, limitations and hopes for the future. *Br J Pharmacol.* 2009;157(2):220–233. doi:10.1111/j.1476-5381.2009.00190.x.
30. Winograd R, Byrne KT, Evans RA, Odorizzi PM, Meyer ARL, Bajor DL, Clendenin C, Stanger BZ, Furth EE, Wherry EJ, et al. Induction of T-cell immunity overcomes complete resistance to PD-1 and CTLA-4 blockade and improves survival in pancreatic carcinoma. *Cancer Immunol Res.* 2015;3(4):399–411. doi:10.1158/2326-6066.CIR-14-0215.
31. Ma Y, Li J, Wang H, Chiu Y, Kingsley CV, Fry D, Delaney SN, Wei SC, Zhang J, Maitra A, et al. Combination of PD-1 inhibitor and OX40 agonist induces tumor rejection and immune memory in mouse models of pancreatic cancer. *Gastroenterol.* 2020;159(1):306–319. doi:10.1053/j.gastro.2020.03.018.
32. Pham TND, Shields MA, Spaulding C, Principe DR, Li B, Underwood PW, Trevino JG, Bentrem DJ, Munshi HG. Preclinical models of pancreatic ductal adenocarcinoma and their utility in immunotherapy studies. *Cancers.* 2021;13(3):440. doi:10.3390/cancers13030440.
33. Butte MJ, Peña-Cruz V, Kim M-J, Freeman GJ, Sharpe AH. Interaction of human PD-L1 and B7-1. *Mol Immunol.* 2008;45(13):3567–3572. doi:10.1016/j.molimm.2008.05.014.
34. Lecis D, Sangaletti S, Colombo MP, Chiodoni C. Immune checkpoint ligand reverse signaling: looking back to go forward in cancer therapy. *Cancers (Basel).* 2019;11(5):624. doi:10.3390/cancers11050624.
35. Nomi T, Sho M, Akahori T, Hamada K, Kubo A, Kanehiro H, Nakamura S, Enomoto K, Yagita H, Azuma M, et al. Clinical significance and therapeutic potential of the programmed death-1 ligand/programmed death-1 pathway in human pancreatic cancer. *Clin Cancer Res.* 2007;13(7):2151–2157. doi:10.1158/1078-0432.CCR-06-2746.
36. Sandin LC, Eriksson F, Ellmark P, Loskog AS, Tötterman TH, Magsbo SM. Local CTLA4 blockade effectively restrains experimental pancreatic adenocarcinoma growth in vivo. *Oncoimmunology.* 2014;3(1):16. doi:10.4161/onci.27614.
37. Luheshi NM, Coates-Ulrichsen J, Harper J, Mullins S, Sulikowski MG, Martin P, Brown L, Lewis A, Davies G, Morrow M, et al. Transformation of the tumour microenvironment by a CD40 agonist antibody correlates with improved responses to PD-L1 blockade in a mouse orthotopic pancreatic tumour model. *Oncotarget.* 2016;7(14):18508–18520. doi:10.18632/oncotarget.7610.
38. Le DT, Durham JN, Smith KN, Wang H, Bartlett BR, Aulakh LK, Lu S, Kemberling H, Wilt C, Lubner BS, et al. Mismatch repair deficiency predicts response of solid tumors to PD-1 blockade. *Science.* 2017;357(6349):409–413. doi:10.1126/science.aan6733.
39. O'Reilly EM, Oh D-Y, Dhani N, Renouf DJ, Lee MA, Sun W, Fisher G, Hezel A, Chang S-C, Vlahovic G, et al. Durvalumab with or without tremelimumab for patients with metastatic pancreatic ductal adenocarcinoma: a phase 2 randomized clinical trial. *JAMA Oncol.* 2019;5(10):1431–1438. doi:10.1001/jamaoncol.2019.1588.
40. Di Marco M, Grassi E, Durante S, Vecchiarelli S, Palloni A, Macchini M, Casadei R, Ricci C, Panzacchi R, Santini D, et al. State of the art biological therapies in pancreatic cancer. *World J Gastrointest Oncol.* 2016 Jan 15;8(1):55–66. doi:10.4251/wjgo.v8.i1.55.
41. Birnbaum DJ, Finetti P, Lopresti A, Gilabert M, Poizat F, Turrini O, Raoul J-L, Delperio J-R, Moutardier V, Birnbaum D, et al. Prognostic value of PDL1 expression in pancreatic cancer. *Oncotarget.* 2016;7(44):71198–71210. doi:10.18632/oncotarget.11685.
42. Liechtenstein T, Perez-Janices N, Blanco-Luquin I, Goyvaerts C, Schwarze J, Dufait I, Lanna A, Ridder MD, Guerrero-Setas D, Breckpot K, et al. Anti-melanoma vaccines engineered to simultaneously modulate cytokine priming and silence PD-L1 characterized using ex vivo myeloid-derived suppressor cells as a readout of therapeutic efficacy. *Oncoimmunology.* 2014;3(7):e945378. doi:10.4161/21624011.2014.945378.
43. Ballbach M, Dannert A, Singh A, Siegmund DM, Handgretinger R, Piali L, Rieber N, Hartl D. Expression of checkpoint molecules on myeloid-derived suppressor cells. *Immunol Lett.* 2017;192:1–6. doi:10.1016/j.imlet.2017.10.001.
44. Pinton L, Solito S, Damuzzo V, Francescato S, Pozzuoli A, Berizzi A, Mocellin S, Rossi CR, Bronte V, Mandruzzato S, et al. Activated T cells sustain myeloid-derived suppressor cell-mediated immune suppression. *Oncotarget.* 2015;7(2):1168–1184. doi:10.18632/oncotarget.6662.
45. Iwata T, Kondo Y, Kimura O, Morosawa T, Fujisaka Y, Umetsu T, Kogure T, Inoue J, Nakagome Y, Shimosegawa T, et al. PD-L1(+) MDSCs are increased in HCC patients and induced by soluble factor in the tumor microenvironment. *Sci Rep.* 2016;6(1):39296. doi:10.1038/srep39296.
46. Thorn M, Guha P, Cunetta M, Espat NJ, Miller G, Junghans RP, Katz SC. Tumor-associated GM-CSF overexpression induces immunoinhibitory molecules via STAT3 in myeloid-suppressor cells infiltrating liver metastases. *Cancer Gene Ther.* 2016;23(6):188. doi:10.1038/cgt.2016.19.
47. Görgün G, Samur MK, Cowens KB, Paula S, Bianchi G, Anderson JE, White RE, Singh A, Ohguchi H, Suzuki R, et al. Lenalidomide enhances immune checkpoint blockade-induced immune response in multiple myeloma. *Clin Cancer Res Off J Am Assoc Cancer Res.* 2015;21(20):4607–4618. doi:10.1158/1078-0432.CCR-15-0200.
48. Chen S, Liu H, Su N, Zhang G, Wang L. Myeloid-derived suppressor cells promote age-related increase of lung cancer growth via B7-H1. *Exp Gerontol.* 2015;61:84–91. doi:10.1016/j.exger.2014.12.001.
49. Sharma V, Dong H, Kwon E, Karnes RJ. Positive pelvic lymph nodes in prostate cancer harbor immune suppressor cells to impair tumor-reactive T cells. *Eur Urol Focus.* 2018;4(1):75–79. doi:10.1016/j.euf.2016.09.003.
50. Zhang Z-N, Yi N, Zhang T-W, Zhang -L-L, Wu X, Liu M, Fu Y-J, He S-J, Jiang Y-J, Ding H-B, et al. Myeloid-derived suppressor cells associated with disease progression in primary HIV infection: PD-L1 blockade attenuates inhibition. *JAIDS J Acq Immune Defic Syndr.* 2017;76(2):200–208. doi:10.1097/QAI.0000000000001471.

51. Mielgo A, Schmid MC. Impact of tumour associated macrophages in pancreatic cancer. *BMB Rep.* 2013;46(3):131–138. doi:10.5483/BMBRep.2013.46.3.036.
52. Knudsen ES, Vail P, Balaji U, Ngo H, Botros IW, Makarov V, Riaz N, Balachandran V, Leach S, Thompson DM, et al. Stratification of pancreatic ductal adenocarcinoma: combinatorial genetic, stromal, and immunologic markers. *Clin Cancer Res Off J Am Assoc Cancer Res.* 2017;23(15):4429–4440. doi:10.1158/1078-0432.CCR-17-0162.
53. Shen L, Gao Y, Liu Y, Zhang B, Liu Q, Wu J, Fan L, Ou Q, Zhang W, Shao L, et al. PD-1/PD-L pathway inhibits M.tb-specific CD4(+) T-cell functions and phagocytosis of macrophages in active tuberculosis. *Sci Rep.* 2016;6(1):38362. doi:10.1038/srep38362.
54. Jiang C, Yuan F, Wang J, Wu L. Oral squamous cell carcinoma suppressed antitumor immunity through induction of PD-L1 expression on tumor-associated macrophages. *Immunobiology.* 2017;222(4):651–657. doi:10.1016/j.imbio.2016.12.002.
55. Komohara Y, Fujiwara Y, Ohnishi K, Takeya M. Tumor-associated macrophages: potential therapeutic targets for anti-cancer therapy. *Adv Drug Deliv Rev.* 2016;99:180–185. doi:10.1016/j.addr.2015.11.009.
56. Harada K, Dong X, Estrella JS, Correa AM, Xu Y, Hofstetter WL, Sudo K, Onodera H, Suzuki K, Suzuki A, et al. Tumor-associated macrophage infiltration is highly associated with PD-L1 expression in gastric adenocarcinoma. *Gastric Cancer.* 2018;21(1):31–40. doi:10.1007/s10120-017-0760-3.
57. Teramoto K, Igarashi T, Kataoka Y, Ishida M, Hanaoka J, Sumimoto H, Daigo Y. Clinical significance of PD-L1-positive cancer-associated fibroblasts in pN0M0 non-small cell lung cancer. *Lung Cancer.* 2019;137:56–63. doi:10.1016/j.lungcan.2019.09.013.
58. Yoshikawa K, Ishida M, Yanai H, Tsuta K, Sekimoto M, Sugie T. Prognostic significance of PD-L1-positive cancer-associated fibroblasts in patients with triple-negative breast cancer. *BMC Cancer.* 2021;21(1):239. doi:10.1186/s12885-021-07970-x.
59. Dominguez CX, Müller S, Keerthivasan S, Koeppen H, Hung J, Gierke S, Breart B, Foreman O, Bainbridge TW, Castiglioni A, et al. Single-cell RNA sequencing reveals stromal evolution into LRRC15 + myofibroblasts as a determinant of patient response to cancer immunotherapy. *Cancer Discov.* 2020;10(2):232–253. doi:10.1158/2159-8290.CD-19-0644.
60. Karakhanova S, Meisel S, Ring S, Mahnke K, Enk AH. ERK/p38 MAP-kinases and PI3K are involved in the differential regulation of B7-H1 expression in DC subsets. *Eur J Immunol.* 2010;40(1):254–266. doi:10.1002/eji.200939289.
61. Gabrilovich DI, Ostrand-Rosenberg S, Bronte V. Coordinated regulation of myeloid cells by tumours. *nature reviews. Immunol.* 2012;12(4):253–268. doi:10.1038/nri3175.
62. Wilcox RA, Feldman AL, Wada DA, Yang -Z-Z, Comfere NI, Dong H, Kwon ED, Novak AJ, Markovic SN, Pittelkow MR, et al. B7-H1 (PD-L1, CD274) suppresses host immunity in T-cell lymphoproliferative disorders. *Blood.* 2009;114(10):2149–2158. doi:10.1182/blood-2009-04-216671.
63. Francisco LM, Salinas VH, Brown KE, Vanguri VK, Freeman GJ, Kuchroo VK, Sharpe AH. PD-L1 regulates the development, maintenance, and function of induced regulatory T cells. *J Exp Med.* 2009;206(13):3015–3029. doi:10.1084/jem.20090847.
64. Yi T, Li X, Yao S, Wang L, Chen Y, Zhao D, Johnston HF, Young JS, Liu H, Todorov I, et al. Host APCs augment in vivo expansion of donor natural regulatory T cells via B7H1/B7.1 in allogeneic recipients. *J Immunol.* 2011;186(5):2739–2749. doi:10.4049/jimmunol.1002939.